Observation of a New Charmed Baryon Decaying to $\Xi_c^+\pi^-\pi^+$

R. Aaij *et al.*[*]
(LHCb Collaboration)

(Received 27 February 2025; revised 24 June 2025; accepted 20 August 2025; published 14 October 2025; corrected 9 December 2025)

The $\Xi_c^+\pi^-\pi^+$ spectrum is investigated using proton-proton collisions at a center-of-mass energy of 13 TeV, corresponding to an integrated luminosity of 5.4 fb^{-1}, collected by the LHCb experiment during 2016–2018. Four states are observed with high significance, and their masses and widths are measured to be $m[\Xi_c(2815)^+] = 2816.65 \pm 0.03 \pm 0.03 \pm 0.23$ MeV, $\Gamma[\Xi_c(2815)^+] = 2.07 \pm 0.08 \pm 0.12$ MeV, $m[\Xi_c(2923)^+] = 2922.8 \pm 0.3 \pm 0.5 \pm 0.2$ MeV, $\Gamma[\Xi_c(2923)^+] = 5.3 \pm 0.9 \pm 1.4$ MeV, $m[\Xi_c(2970)^+] = 2968.6 \pm 0.5 \pm 0.5 \pm 0.2$ MeV, $\Gamma[\Xi_c(2970)^+] = 31.7 \pm 1.7 \pm 1.9$ MeV, $m[\Xi_c(3080)^+] = 3076.8 \pm 0.7 \pm 1.3 \pm 0.2$ MeV, $\Gamma[\Xi_c(3080)^+] = 6.8 \pm 2.3 \pm 0.9$ MeV, where the uncertainties are statistical, systematic, and due to the limited precision on the Ξ_c^+ mass, respectively. The $\Xi_c(2923)^+$ baryon is observed for the first time, and is consistent with being the isospin partner of the previously observed $\Xi_c(2923)^0$ state. Most of the measured parameters are more precise than existing world averages.

DOI: 10.1103/gghl-m6fm

Singly charmed baryons are bound states of a charm quark (c) and two light quarks (u, d, or s). Because of the large mass difference between the charm and the lighter quarks, these baryons provide an insight into the spectrum of hadronic states using symmetries described by the heavy quark effective theory [1,2]. Numerous theoretical predictions of the properties of heavy baryons, containing either a charm or a beauty quark, have been made in recent years [3–26], including some based on lattice QCD calculations [27–30]. There are 15 singly charmed baryons with orbital angular momentum $L = 0$, all of which have now been observed [31]. The number increases drastically when considering the orbital and radial excitations. Modeling such states as a heavy quark interacting with a light diquark can help restrict the number of possible physical states [16,20]. However, despite the progress made in recent years, this number remains much higher than that observed experimentally [32–37]. This implies that many other states remain undiscovered or that some configurations are forbidden by selection rules. The latter would have a broad impact in hadron spectroscopy given that the diquark is also used as a building block of exotic states, including tetraquarks and pentaquarks [38–40].

The Ξ_c baryons, states with quark content $c\,s\,u$ or $c\,s\,d$, are described by a wave function that is antisymmetric (e.g., the Ξ_c ground state) or symmetric [e.g., Ξ_c' or $\Xi_c(2645)$ excitations] under interchange of the light quark flavors. More than 100 excited Ξ_c baryons are expected in the mass region 2.8–3.8 GeV [27] and the mass splitting between the states can be so small, relative to their natural widths, that they are difficult to resolve experimentally. (Natural units with $\hbar = c = 1$ are used throughout.) This might be the case for the $\Xi_c(2970)$ state whose natural width was measured to be about 30 MeV in the $\Xi_c'\,\pi$ and $\Xi_c\pi^+\pi^-$ spectra [41] while only 15 MeV in the $\Lambda_c^+\,K^-\,\pi^+$ [42] and $\Lambda_c^+\,K^-$ [36] systems. More precise measurements are needed to determine if two different Ξ_c baryons have been mistakenly identified as a single state due to the proximity of their masses.

This Letter presents a search for excited Ξ_c^+ baryons, hereafter collectively termed Ξ_c^{**+}, in the $\Xi_c^+\,\pi^-\,\pi^+$ spectrum. This final state was studied by the Belle Collaboration, which reported the observation of the $\Xi_c(2815)^+$ and $\Xi_c(2970)^+$ baryons [41]. The spin parity of the latter was also measured to be $J^P = \frac{1}{2}^+$ [43]. A further structure peaking at around 2.92 GeV was noted, although it was not statistically significant.

Data used in this analysis were collected by the LHCb experiment during 2016–2018 from proton-proton collisions at a center-of-mass energy of 13 TeV, corresponding to an integrated luminosity of 5.4 fb^{-1}. Excited Ξ_c^+ states are reconstructed through their intermediate decay to $\Xi_c(2645)^0\pi^+$, with $\Xi_c(2645)^0 \to \Xi_c^+\pi^-$ and $\Xi_c^+ \to pK^-\pi^+$. (The inclusion of charge-conjugate processes is implied throughout.)

The LHCb detector [44,45] is a single-arm forward spectrometer covering the pseudorapidity range $2 < \eta < 5$, designed for the study of particles containing b or c quarks. The detector elements particularly relevant to this analysis

[*]Full author list given at the end of the Letter.

are a silicon-strip vertex detector surrounding the proton-proton interaction region that allows c and b hadrons to be identified from their characteristically long flight distance [46]; a large-area silicon-strip detector located upstream of a dipole magnet with a bending power of about 4 T m, and three stations of silicon-strip detectors and straw drift tubes [47] placed downstream of the magnet; and two ring-imaging Cherenkov detectors that provide particle identification (PID) information to discriminate between different species of charged hadrons [48]. The online event selection is performed by a trigger [49] consisting of a hardware stage based on information from the calorimeter and muon systems, followed by a two-level software stage that applies a full event reconstruction.

Simulation is used in this analysis to optimize the event selection and to model the experimental mass resolution. Proton-proton collisions are generated using PYTHIA [50] with a specific LHCb configuration [51]. Decays of unstable particles are described by EvtGen [52]. The interaction of the generated particles with the detector, and its response, are implemented using the Geant4 toolkit [53] as described in Ref. [54].

In order to maximize the signal efficiency, no explicit requirements are imposed at the hardware trigger stage. At the software trigger stage a dedicated algorithm reconstructs $\Xi_c^+ \to pK^-\pi^+$ candidates from the combination of three reconstructed tracks that must fulfill loose kinematic and PID requirements [55] and be consistent with originating from a common vertex with significant displacement from any primary interaction vertex (PV) in the event. The Ξ_c^+ candidate must have a measured lifetime with respect to the associated PV exceeding 0.15 ps, and a mass in the range $2432.5 < m(pK^-\pi^+) < 2502.5$ MeV.

The Ξ_c^+ candidates selected by the trigger are subsequently combined with a pair of oppositely charged particles, fulfilling loose pion PID requirements and consistent with originating from the Ξ_c^+ associated PV, to form $\Xi_c^{**+} \to \Xi_c(2645)^0(\to \Xi_c^+\pi^-)\pi^+$ candidates. The $\Xi_c^+\,\pi^-\,\pi^+$ system must form a good-quality vertex and satisfy the reconstructed mass conditions $m(\Xi_c^+\pi^-\pi^+) < 3300$ MeV and $[m(\Xi_c^+\pi^-) - m(\Xi_c^+) - m_{\pi^-}^{\rm PDG}] < 150$ MeV, where the second condition selects the $\Xi_c(2645)^0$ resonance region and $m_{\pi^-}^{\rm PDG}$ is the known pion mass taken from the Particle Data Group [31].

Three selection stages are performed to sequentially optimize the signal for Ξ_c^+, $\Xi_c(2645)^0$, and Ξ_c^{**+} states. More information on each stage is included in the End Matter. In the first (Ξ_c^+) selection stage, a series of loose criteria are initially imposed to reduce the dominant combinatorial background by 85% while retaining 83% of the signal. These include a requirement on the alignment of the Ξ_c^+ momentum with the direction determined by its production and decay vertices, PID requirements on each final-state particle, and loose requirements on topological variables related to the Ξ_c^+ flight distance and its consistency with originating from a PV.

To further suppress background in the Ξ_c^+ sample, a multivariate algorithm (MVA) is trained with signal and background samples extracted using the sPlot technique [56]. The Ξ_c^+ mass distribution is fitted to obtain weights for signal and background, based on a 5% random sampling of the full data sample. In this fit the signal is described by a double Gaussian function, i.e., the sum of two Gaussian functions constrained to have a common mean, and the background by a first-order polynomial function. A cross-validation method is used to ensure the classifier is not applied to the data on which it is trained. A feed-forward neural network [57,58] is configured with a loss function that properly accounts for the weights in the training samples [59]. A total of 29 input variables are included, mainly topological quantities and PID variables for the final-state particles. Following the training, a requirement is imposed on the classifier output to maximize the signal significance $S/\sqrt{S+B}$, where S (B) is the signal (background) yield. This selection retains 84% (16%) of the signal (background). The resulting $m(pK^-\pi^+)$ distribution, after imposing all Ξ_c^+ selection criteria, is shown in Fig. 1 for the full data sample. Also shown is an indicative fit using the same model as described above. For subsequent analysis a tighter mass window of $2451.3 < m(pK^-\pi^+) < 2486.0$ MeV is imposed, containing 98% of the signal. Around 7.7×10^6 Ξ_c^+ signal candidates are selected, with a purity of 84%.

In the second selection stage, a separate classifier is trained to optimize the signal significance of the $\Xi_c(2645)^0$ state. The signal and background training samples are again derived from cross-validated data using the sPlot technique [56], following a fit to the quantity $m_{\rm corr}[\Xi_c(2645)^0] \equiv m(\Xi_c^+\pi^-) - m(\Xi_c^+) + m_{\Xi_c^+}^{\rm PDG}$, where

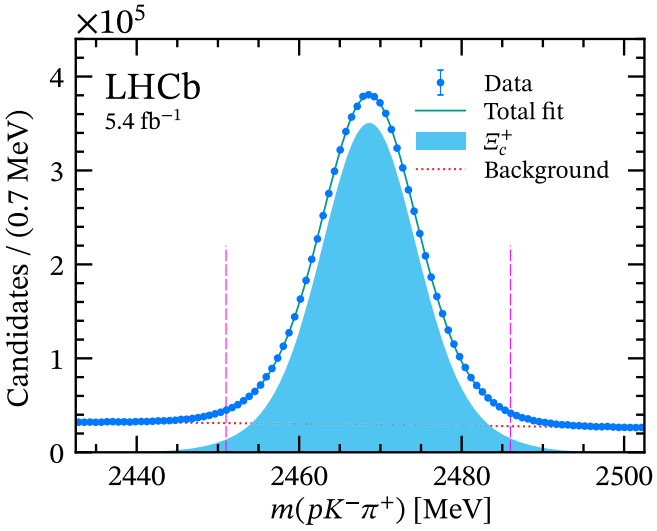

FIG. 1. Distribution of $m(pK^-\pi^+)$ for candidates passing Ξ_c^+ selection requirements, together with the fit model. The dashed vertical lines delimit the mass window imposed for subsequent selection stages.

the final entry corresponds to the known Ξ_c^+ mass [31]. Using this mass difference leads to improved resolution and, hence, higher signal purity. In the fit, the $\Xi_c(2645)^0$ signal peak is described by the convolution of a relativistic Breit-Wigner (RBW) function with a double Gaussian resolution function. Simulation is used to fix the parameters of the resolution function, with both widths free to vary in the fit through a common scale factor to account for possible mismodeling. The dominant background is combinatorial, either from genuine Ξ_c^+ baryons combined with an unrelated track, or fake Ξ_c^+ candidates. These components are described empirically by a function $f(x) = a(x-m_0)^k + b(x-m_0)$ with a, b, k, and m_0 as free parameters. Two additional peaking backgrounds are observed in the sample. The first occurs close to the signal peak, originating from $\Xi_c(2815)^0 \to \Xi_c(2645)^+(\to \Xi_c^+\pi^0)\pi^-$ decays, where the neutral pion is not reconstructed. The second occurs in the mass region around 2680 MeV, due to $\Xi_c(2790)^0 \to \Xi_c'^+(\to \Xi_c^+\gamma)\pi^-$ decays with the photon not reconstructed. Both of these partially reconstructed backgrounds are described using templates derived from a fast simulation software [60]. Their mass positions are allowed to shift through Gaussian constraints centered on zero and with widths 0.3 MeV and 0.5 MeV for the $\Xi_c(2815)^0$ and $\Xi_c(2790)^0$ decays, respectively, based on the experimental mass uncertainties of these states [31].

The weighted signal and background samples obtained from the sPlot fit are used to train a gradient boosted decision tree (BDT) [61–63] with 14 input variables, one of which is the neural network output from the first selection stage. The other variables include PID and kinematic quantities for the pion, and topological quantities characterizing the $\Xi_c^+\,\pi^-$ vertex quality. A requirement is imposed on the BDT output to optimize the signal significance, which gives a signal (background) retention of 95% (74%). A mass requirement $2635 < m_{\rm corr}[\Xi_c(2645)^0] < 2656$ MeV is then applied, containing 98% of the signal candidates. In total, around 56.5×10^4 $\Xi_c(2645)^0$ signal candidates are selected, with a purity of 52%. The mass distribution after all criteria have been imposed is shown in Fig. 2 along with the results of an illustrative fit with the same model as described above.

The final selection stage uses a third MVA to optimize possible Ξ_c^{**+} signal peaks in an unbiased way. Simulation is used as a proxy for the signal to train the classifier, with four samples generated with Ξ_c^{**+} mass assignments 2815, 2923, 2970, and 3055 MeV. The input variable distributions and classifier performance are similar for the different mass values, so these four samples are combined in the training. The background proxy sample is taken from data, combining the wrong-sign final states $\Xi_c^+\pi^+\pi^-$ and $\Xi_c^+\,\pi^-\,\pi^-$, which is found to provide a good description of the background entering the signal sample. A gradient BDT [64] is trained with 15 input variables covering kinematic, topological, and PID quantities. Following training,

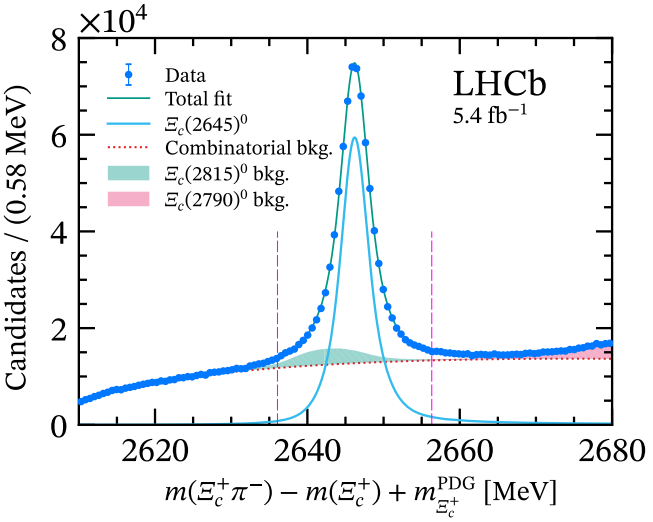

FIG. 2. Distribution of $m_{\rm corr}[\Xi_c(2645)^0]$ for candidates passing the second selection stage. The fit model is also shown for illustrative purposes. The dashed vertical lines enclose the mass region selected for subsequent analysis.

a requirement on the BDT output is imposed to maximize the quantity $\varepsilon/(5/2+\sqrt{B})$ [65], where ε is the signal efficiency taken from simulation and B is the background yield under the signal peak of interest, taken from the wrong-sign sample. The optimal requirement is calculated separately for the four mass assignments used in simulation, and exhibits a weak mass dependence. The chosen requirement is based on the $\Xi_c(2923)^+$ hypothesis, and retains 34% of signal while rejecting 99.3% of background in the proxy samples.

A final requirement is imposed to reject cases where a single particle is reconstructed as two tracks, with both included in the final state. Such candidates are removed by requiring the two-dimensional angular separation between all pairs of final-state particles to exceed 0.08 mrad. Following the application of all selection criteria, 84% of events include only one selected Ξ_c^{**+} candidate. For events with multiple candidates, all are accepted, with an alternative treatment considered later as a cross-check.

The mass distribution for candidates passing all selection requirements is shown in Fig. 3, expressed in terms of the mass difference $\Delta M \equiv m(\Xi_c^+\pi^-\pi^+) - m(\Xi_c^+) - 2m_{\pi^\pm}^{\rm PDG}$. Four distinct peaks are observed above a smooth background rising from the kinematic threshold. These peaks are labeled as $\Xi_c(2815)^+$, $\Xi_c(2923)^+$, $\Xi_c(2970)^+$, and $\Xi_c(3080)^+$ based on their proximity to existing states [31], or in the case of $\Xi_c(2923)^+$ to the corresponding neutral state observed in decays to $\Lambda_c^+K^-$ [36].

An extended unbinned maximum-likelihood fit is performed on the ΔM distribution to determine the masses and widths of these states, and their statistical significances. In this fit, the background is described by an empirical function $f(x) = x^k\exp(-cx)$, where $x \equiv (\Delta M - m_0)$,

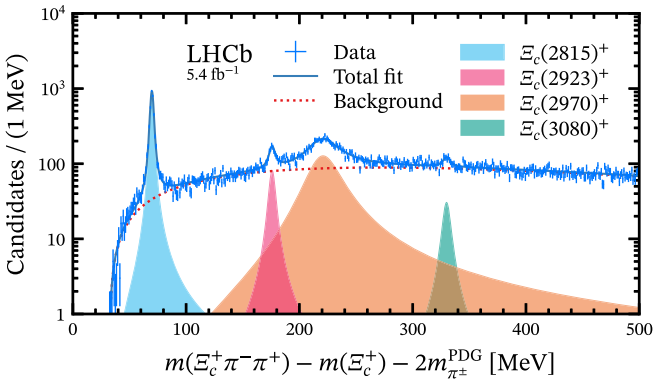

FIG. 3. Distribution of ΔM for candidates passing all selection requirements, shown with the fit model. The individual signal components for the four observed states are drawn separately as filled curves, and the background as a dotted line.

and k, c, and m_0 are free parameters. This model choice is motivated by studies of the wrong-sign samples, giving a compromise between a good fit quality and a small number of free parameters. Each signal peak is described by the convolution of a relativistic Breit-Wigner function with a resolution function obtained from simulation. Different assumptions are tested for the Blatt-Weisskopf barrier factors [66] and orbital angular momentum of the states, with the results used to assign systematic uncertainties as described later. The resolution function is determined using the four simulated Ξ_c^{**+} samples, which correspond quite closely in mass to the states observed in data. The ΔM resolution is determined from simulation, and is described by a double Gaussian function with a mass-dependent scale factor applied to both widths. This resolution varies from 1 MeV for the $\Xi_c(2815)^+$ state to 2.5 MeV for the $\Xi_c(3080)^+$ state.

The free parameters of the ΔM fit are the yields (N), peak positions, and widths (Γ) of each of the four signal peaks, the three background shape parameters, and the background yield. The absolute masses (m) are then determined from the peak positions in ΔM by adding the known Ξ_c^+ and $\pi^\pm$ masses [31]. The fit model provides a good description of the data, with a χ^2 of 478 for 458 degrees of freedom. The parameters for the observed states are measured to be

$$
\begin{aligned}
N[\Xi_c(2815)^+] &= 4072 \pm 77, \\
m[\Xi_c(2815)^+] &= 2816.65 \pm 0.03 \pm 0.03 \pm 0.23\ \text{MeV}, \\
\Gamma[\Xi_c(2815)^+] &= 2.07 \pm 0.08 \pm 0.12\ \text{MeV}, \\
N[\Xi_c(2923)^+] &= 738 \pm 76, \\
m[\Xi_c(2923)^+] &= 2922.8 \pm 0.3 \pm 0.5 \pm 0.2\ \text{MeV}, \\
\Gamma[\Xi_c(2923)^+] &= 5.3 \pm 0.9 \pm 1.4\ \text{MeV}, \\
N[\Xi_c(2970)^+] &= 6105 \pm 255, \\
m[\Xi_c(2970)^+] &= 2968.6 \pm 0.5 \pm 0.5 \pm 0.2\ \text{MeV}, \\
\Gamma[\Xi_c(2970)^+] &= 31.7 \pm 1.7 \pm 1.9\ \text{MeV}, \\
N[\Xi_c(3080)^+] &= 344 \pm 77, \\
m[\Xi_c(3080)^+] &= 3076.8 \pm 0.7 \pm 1.3 \pm 0.2\ \text{MeV}, \\
\Gamma[\Xi_c(3080)^+] &= 6.8 \pm 2.3 \pm 0.9\ \text{MeV},
\end{aligned}
$$

where the first uncertainty is statistical, the second is due to experimental systematic effects discussed below, and the third uncertainty on the masses is from the limited knowledge of the Ξ_c^+ mass [31].

The statistical significance for the two lowest-yield peaks is determined from Wilks' theorem [67]. The $\Xi_c(2923)^+$ state is observed with over 10σ significance, representing the discovery of this state. The $\Xi_c(3080)^+$ state is observed with 5.4σ significance. To account for possible systematic effects from the choice of signal and background model, the calculation is repeated for the alternative model choices described below, and the lowest significance is quoted.

Various sources of systematic uncertainty are considered for the mass and width measurements, as summarized in Table I. Alternative descriptions of the signal peaks are tested by varying the Blatt-Weisskopf radius used in the RBW function from its baseline value of 3.1 GeV^{-1} to 2.0 and 4.0 GeV^{-1}. In addition, the assumed orbital angular momentum of the decay products, L, is varied independently for all four observed states to cover any physically allowed values between $L = 0$ and $L = 2$. The standard

TABLE I. Summary of uncertainties on all measured parameters (in MeV), including a breakdown of systematic uncertainties as described in the text. Blank entries are not relevant for that measurement.

	$\Xi_c(2815)^+$		$\Xi_c(2923)^+$		$\Xi_c(2970)^+$		$\Xi_c(3080)^+$	
Contribution	m	Γ	m	Γ	m	Γ	m	Γ
RBW	0.00	0.02	0.09	1.12	0.15	0.55	0.02	0.68
Interference	0.00	0.01	0.53	0.70	0.44	1.05	1.26	0.65
Resolution	0.00	0.12	0.00	0.11	0.01	0.04	0.00	0.08
Background	0.00	0.01	0.01	0.32	0.11	1.51	0.04	0.08
Momentum scale	0.02		0.05		0.07		0.10	
Energy loss	0.02		0.02		0.02		0.02	
Selection bias	0.02		0.02		0.02		0.02	
Total systematic	0.03	0.12	0.54	1.36	0.48	1.92	1.27	0.95
Statistical	0.03	0.08	0.28	0.87	0.46	1.68	0.72	2.28

deviation of each signal parameter across the full ensemble of alternative signal models is taken as a systematic uncertainty (labeled "RBW" in Table I). In the baseline fit no interference is included between the observed states. The $\Xi_c(2970)^+$ resonance has a significant overlap with both the $\Xi_c(2923)^+$ and $\Xi_c(3080)^+$ peaks, and so any interference could influence the measured parameters. This is tested by performing two additional fits, independently allowing interference between each pair of adjacent states, and assigning a systematic uncertainty equal to the maximum shift in each parameter compared to the baseline result ("Interference").

Potential mismodeling of the detector resolution in simulation is tested by multiplying the Gaussian widths for all resolution functions by a scale factor of 0.9 or 1.1 and repeating the fits. This range is chosen based on detailed studies of the $\Xi_c^+(2645)$ peak in data and simulation. Systematic uncertainties on fit parameters are then assigned as their maximum shifts ("Resolution"). The description of the background component in the fit to the Δm distribution is varied by using a third-order polynomial function, and associated systematic uncertainties are assigned as the shift in fit parameters from their baseline values ("Background").

The mass measurements may be affected by the LHCb momentum scale calibration ("Momentum scale") and by mismodeling of material leading to incorrect energy loss assumptions in simulation and particle reconstruction ("Energy loss"). Previous studies indicate that the former effect is associated with a systematic uncertainty corresponding to 0.03% of the Q value for the decay [68]. The systematic uncertainty due to imperfect modeling of the energy loss is assigned as 0.02 MeV for all mass measurements, corresponding to 0.01 MeV for each of the two pion tracks entering the ΔM calculation [68]. The impact from other final-state particles cancels in the mass difference. In addition, a potential bias in the mass measurements originating from the event selection is tested by comparing the reconstructed masses in simulation before and after the offline selection requirements are imposed. A small shift of 0.016 MeV is found, consistent for all four states, which is assigned as a systematic uncertainty ("Selection bias"). No correction is applied as this shift is found to be compatible with zero.

Several cross-checks are performed to confirm the robustness of the results. The fit is repeated separately for each of the two $\Xi_c^\pm$ charges, for each of the two LHCb dipole magnet polarities, and for each of the three data-taking years. In all cases the results are self-consistent. Fits are also performed with additional resonances allowed to contribute, namely $\Xi_c(2939)^+$, $\Xi_c(3055)^+$, and $\Xi_c(3123)^+$ states. These are added individually to the fit, with their masses and widths constrained from external measurements [31]. In all cases the results are stable compared to the baseline fit, and no evidence is found for the presence of these extra states in the data sample.

In conclusion, this Letter presents a search for excited Ξ_c^+ states decaying to $\Xi_c(2645)^0\pi^+$, with $\Xi_c(2645)^0 \to \Xi_c^+\pi^-$ and $\Xi_c^+ \to pK^-\pi^+$. Four states are observed with high significance, including the discovery of the $\Xi_c(2923)^+$ baryon, and the first observation of the $\Xi_c(3080)^+$ baryon in this final state. Masses and widths are measured for all four states, and are competitive with, or more precise than the existing world averages. The natural width of the $\Xi_c(2970)^+$ state is not consistent with that of the $\Xi_c(2965)^0$ baryon observed in the $\Lambda_c^+ K^-$ mass spectrum [36], indicating that the two are different excited Ξ_c states. This continues the success of the LHCb experiment in discovering new hadronic states and precisely measuring their properties, a key input for understanding QCD in the nonperturbative realm.

Acknowledgments—We express our gratitude to our colleagues in the CERN accelerator departments for the excellent performance of the LHC. We thank the technical and administrative staff at the LHCb institutes. We acknowledge support from CERN and from the national agencies: ARC (Australia); CAPES, CNPq, FAPERJ, and

FINEP (Brazil); MOST and NSFC (China); CNRS/IN2P3 (France); BMBF, DFG, and MPG (Germany); INFN (Italy); NWO (Netherlands); MNiSW and NCN (Poland); MCID/IFA (Romania); MICIU and AEI (Spain); SNSF and SER (Switzerland); NASU (Ukraine); STFC (United Kingdom); DOE NP and NSF (USA). We acknowledge the computing resources that are provided by ARDC (Australia), CBPF (Brazil), CERN, IHEP, and LZU (China), IN2P3 (France), KIT and DESY (Germany), INFN (Italy), SURF (Netherlands), Polish WLCG (Poland), IFIN-HH (Romania), PIC (Spain), CSCS (Switzerland), and GridPP (United Kingdom). We are indebted to the communities behind the multiple open-source software packages on which we depend. Individual groups or members have received support from Key Research Program of Frontier Sciences of CAS, CAS PIFI, CAS CCEPP, Fundamental Research Funds for the Central Universities, and Science and Technology Program of Guangzhou (China); Minciencias (Colombia); EPLANET, Marie Skłodowska-Curie Actions, ERC, and NextGenerationEU (European Union); A*MIDEX, ANR, IPhU, and Labex P2IO, and Région Auvergne-Rhône-Alpes (France); Alexander-von-Humboldt Foundation (Germany); ICSC (Italy); Severo Ochoa and María de Maeztu Units of Excellence, GVA, XuntaGal, GENCAT, InTalent-Inditex, and Prog. Atracción Talento CM (Spain); SRC (Sweden); the Leverhulme Trust, the Royal Society and UKRI (United Kingdom).

Data availability—The data that support the findings of this Letter are openly available [69].

[1] A. G. Grozin, Introduction to the heavy quark effective theory. Part 1, arXiv:hep-ph/9908366.
[2] T. Mannel, Effective theory for heavy quarks, Lect. Notes Phys. **479**, 387 (1997).
[3] S. Migura, D. Merten, B. Metsch, and H.-R. Petry, Charmed baryons in a relativistic quark model, Eur. Phys. J. A **28**, 41 (2006).
[4] D. Ebert, R. N. Faustov, and V. O. Galkin, Masses of excited heavy baryons in the relativistic quark-diquark model, Phys. Lett. B **659**, 612 (2008).
[5] W. Roberts and M. Pervin, Heavy baryons in a quark model, Int. J. Mod. Phys. A **23**, 2817 (2008).
[6] H. Garcilazo, J. Vijande, and A. Valcarce, Faddeev study of heavy baryon spectroscopy, J. Phys. G **34**, 961 (2007).
[7] A. Valcarce, H. Garcilazo, and J. Vijande, Towards an understanding of heavy baryon spectroscopy, Eur. Phys. J. A **37**, 217 (2008).
[8] D. Ebert, R. N. Faustov, and V. O. Galkin, Spectroscopy and Regge trajectories of heavy baryons in the relativistic quark-diquark picture, Phys. Rev. D **84**, 014025 (2011).
[9] J. Vijande, A. Valcarce, T. F. Caramés, and H. Garcilazo, Heavy hadron spectroscopy: A quark model perspective, Int. J. Mod. Phys. E **22**, 1330011 (2013).
[10] T. Yoshida, E. Hiyama, A. Hosaka, M. Oka, and K. Sadato, Spectrum of heavy baryons in the quark model, Phys. Rev. D **92**, 114029 (2015).
[11] H.-X. Chen, W. Chen, Q. Mao, A. Hosaka, X. Liu, and S.-L. Zhu, P-wave charmed baryons from QCD sum rules, Phys. Rev. D **91**, 054034 (2015).
[12] Z. Shah, K. Thakkar, A. K. Rai, and P. C. Vinodkumar, Mass spectra and Regge trajectories of Λ_c^+, Σ_c^0, Ξ_c^0 and Ω_c^0 baryons, Chin. Phys. C **40**, 123102 (2016).
[13] H.-X. Chen, Q. Mao, A. Hosaka, X. Liu, and S.-L. Zhu, D-wave charmed and bottomed baryons from QCD sum rules, Phys. Rev. D **94**, 114016 (2016).
[14] J. Oudichhya, K. Gandhi, and A. K. Rai, Ground and excited state masses of Ω_c^0, Ω_{cc}^+ and Ω_{ccc}^{++} baryons, Phys. Rev. D **103**, 114030 (2021).
[15] P. Jakhad, J. Oudichhya, K. Gandhi, and A. K. Rai, Identification of newly observed singly charmed baryons using the relativistic flux tube model, Phys. Rev. D **108**, 014011 (2023).
[16] H. García-Tecocoatzi, A. Giachino, J. Li, A. Ramirez-Morales, and E. Santopinto, Strong decay widths and mass spectra of charmed baryons, Phys. Rev. D **107**, 034031 (2023).
[17] E. Ortiz-Pacheco and R. Bijker, Masses and radiative decay widths of S- and P-wave singly, doubly, and triply heavy charm and bottom baryons, Phys. Rev. D **108**, 054014 (2023).
[18] Z.-Y. Li, G.-L. Yu, Z.-G. Wang, and J.-Z. Gu, Heavy quark dominance in orbital excitation of singly and doubly heavy baryons, Eur. Phys. J. C **84**, 106 (2024).
[19] X.-Z. Weng, W.-Z. Deng, and S.-L. Zhu, Heavy baryons in the relativized quark model with chromodynamics, Phys. Rev. D **110**, 056052 (2024).
[20] H. García-Tecocoatzi, A. Giachino, A. Ramirez-Morales, A. Rivero-Acosta, E. Santopinto, and C. A. Vaquera-Araujo, Strong decay widths and mass spectra of the 1D, 2P and 2S singly bottom baryons, Phys. Rev. D **110**, 114005 (2024).
[21] H.-M. Yang and H.-X. Chen, *P*-wave charmed baryons of the $SU(3)$ flavor 6_F, Phys. Rev. D **104**, 034037 (2021).
[22] H.-M. Yang, H.-X. Chen, and Q. Mao, Excited Ξ_c^0 baryons within the QCD sum rule approach, Phys. Rev. D **102**, 114009 (2020).
[23] Q. X. Yu, R. Pavao, V. R. Debastiani, and E. Oset, Description of the Ξ_c and Ξ_b states as molecular states, Eur. Phys. J. C **79**, 167 (2019).
[24] J. Nieves, R. Pavao, and L. Tolos, Ξ_c and Ξ_b excited states within a $SU(6)_{lsf} \times$ HQSS model, Eur. Phys. J. C **80**, 22 (2020).
[25] H. Zhu, N. Ma, and Y. Huang, Description of the newly observed Ξ_c^0 states as molecular states, Eur. Phys. J. C **80**, 1184 (2020).
[26] Z.-G. Wang, The $\Lambda_c(2860)$, $\Lambda_c(2880)$, $\Xi_c(3055)$ and $\Xi_c(3080)$ as D-wave baryon states in QCD, Nucl. Phys. **B926**, 467 (2018).
[27] M. Padmanath, R. G. Edwards, N. Mathur, and M. Peardon, Excited-state spectroscopy of singly, doubly and triply-charmed baryons from lattice QCD, in *Proceedings, 6th International Workshop on Charm Physics (Charm 2013): Manchester, UK, 2013* (2013), arXiv:1311.4806.
[28] M. Padmanath and N. Mathur, Quantum numbers of recently discovered Ω_c^0 baryons from lattice QCD, Phys. Rev. Lett. **119**, 042001 (2017).

[29] Y.-C. Chen and T.-W. Chiu (TWQCD Collaboration), Lattice QCD with $N_f = 2 + 1 + 1$ domain-wall quarks, Phys. Lett. B **767**, 193 (2017).
[30] H. Bahtiyar *et al.* (TRJQCD Collaboration), Charmed baryon spectrum from lattice QCD near the physical point, Phys. Rev. D **102**, 054513 (2020).
[31] S. Navas *et al.* (Particle Data Group), Review of particle physics, Phys. Rev. D **110**, 030001 (2024).
[32] R. Aaij *et al.* (LHCb Collaboration), Study of the $D^0 p$ amplitude in $\Lambda_b^0 \to D^0 p \pi^-$ decays, J. High Energy Phys. 05 (2017) 030.
[33] R. Aaij *et al.* (LHCb Collaboration), Observation of five new narrow Ω_c^0 states decaying to $\Xi_c^+ K^-$, Phys. Rev. Lett. **118**, 182001 (2017).
[34] J. Yelton *et al.* (Belle Collaboration), Observation of excited Ω_c charmed baryons in $e^+ e^-$ collisions, Phys. Rev. D **97**, 051102 (2018).
[35] Y. B. Li *et al.* (Belle Collaboration), Observation of $\Xi_c(2930)^0$ and updated measurement of $B^- \to K^- \Lambda_c^+ \bar{\Lambda}_c^-$ at Belle, Eur. Phys. J. C **78**, 252 (2018).
[36] R. Aaij *et al.* (LHCb Collaboration), Observation of new Ξ_c^0 baryons decaying to $\Lambda_c^+ K^-$, Phys. Rev. Lett. **124**, 222001 (2020).
[37] R. Aaij *et al.* (LHCb Collaboration), Observation of new Ω_c^0 states decaying to the $\Xi_c^+ K^-$ final state, Phys. Rev. Lett. **131**, 131902 (2023).
[38] R. L. Jaffe, Multiquark hadrons. I. Phenomenology of $Q^2 \bar{Q}^2$ mesons, Phys. Rev. D **15**, 267 (1977).
[39] R. L. Jaffe, Multiquark hadrons. II. Methods, Phys. Rev. D **15**, 281 (1977).
[40] L. Maiani, F. Piccinini, A. D. Polosa, and V. Riquer, Diquark-antidiquarks with hidden or open charm and the nature of X(3872), Phys. Rev. D **71**, 014028 (2005).
[41] J. Yelton *et al.* (Belle Collaboration), Study of excited Ξ_c states decaying into Ξ_c^0 and Ξ_c^+ baryons, Phys. Rev. D **94**, 052011 (2016).
[42] Y. Kato *et al.* (Belle Collaboration), Search for doubly charmed baryons and study of charmed strange baryons at Belle, Phys. Rev. D **89**, 052003 (2014).
[43] T. J. Moon *et al.* (Belle Collaboration), First determination of the spin and parity of the charmed-strange baryon $\Xi_c(2970)^+$, Phys. Rev. D **103**, L111101 (2021).
[44] A. A. Alves, Jr. *et al.* (LHCb Collaboration), The LHCb detector at the LHC, J. Instrum. **3**, S08005 (2008).
[45] LHCb Collaboration, LHCb detector performance, Int. J. Mod. Phys. A **30**, 1530022 (2015).
[46] R. Aaij *et al.*, Performance of the LHCb vertex locator, J. Instrum. **9**, P09007 (2014).
[47] P. d'Argent *et al.*, Improved performance of the LHCb outer tracker in LHC Run 2, J. Instrum. **12**, P11016 (2017).
[48] M. Adinolfi *et al.*, Performance of the LHCb RICH detector at the LHC, Eur. Phys. J. C **73**, 2431 (2013).
[49] R. Aaij *et al.*, The LHCb trigger and its performance in 2011, J. Instrum. **8**, P04022 (2013).
[50] T. Sjöstrand, S. Mrenna, and P. Skands, A brief introduction to PYTHIA 8.1, Comput. Phys. Commun. **178**, 852 (2008); T. Sjöstrand, S. Mrenna, and P. Skands, PYTHIA 6.4 physics and manual, J. High Energy Phys. 05 (2006) 026.
[51] I. Belyaev *et al.*, Handling of the generation of primary events in Gauss, the LHCb simulation framework, J. Phys. Conf. Ser. **331**, 032047 (2011).
[52] D. J. Lange, The EvtGen particle decay simulation package, Nucl. Instrum. Methods Phys. Res., Sect. A **462**, 152 (2001).
[53] J. Allison *et al.* (Geant4 Collaboration), Geant4 developments and applications, IEEE Trans. Nucl. Sci. **53**, 270 (2006); S. Agostinelli *et al.* (Geant4 Collaboration), Geant4: A simulation toolkit, Nucl. Instrum. Methods Phys. Res., Sect. A **506**, 250 (2003).
[54] M. Clemencic, G. Corti, S. Easo, C. R. Jones, S. Miglioranzi, M. Pappagallo, and P. Robbe, The LHCb simulation application, Gauss: Design, evolution and experience, J. Phys. Conf. Ser. **331**, 032023 (2011).
[55] A. Papanestis and C. D'Ambrosio (LHCb RICH Collaboration), Performance of the LHCb RICH detectors during the LHC Run II, Nucl. Instrum. Methods Phys. Res., Sect. A **876**, 221 (2017).
[56] M. Pivk and F. R. Le Diberder, *sPlot*: A statistical tool to unfold data distributions, Nucl. Instrum. Methods Phys. Res., Sect. A **555**, 356 (2005).
[57] M. Abadi *et al.*, TensorFlow: Large-scale machine learning on heterogeneous systems, Software available from https://www.tensorflow.org/ (2015).
[58] F. Chollet *et al.*, Keras, https://keras.io (2015).
[59] M. Borisyak and N. Kazeev, Machine learning on data with sPlot background subtraction, J. Instrum. **14**, P08020 (2019).
[60] G. A. Cowan, D. C. Craik, and M. D. Needham, RapidSim: An application for the fast simulation of heavy-quark hadron decays, Comput. Phys. Commun. **214**, 239 (2017).
[61] L. Breiman, J. H. Friedman, R. A. Olshen, and C. J. Stone, *Classification and Regression Trees* (Wadsworth International Group, Belmont, California, USA, 1984).
[62] Y. Freund and R. E. Schapire, A decision-theoretic generalization of on-line learning and an application to boosting, J. Comput. Syst. Sci. **55**, 119 (1997).
[63] F. Pedregosa *et al.*, SCIKIT-LEARN: Machine learning in Python-, J. Mach. Learn. Res. **12**, 2825 (2011), https://jmlr.org/papers/v12/pedregosa11a.html.
[64] L. Prokhorenkova *et al.*, Catboost: Unbiased boosting with categorical features, arXiv:1706.09516.
[65] G. Punzi, Sensitivity of searches for new signals and its optimization, eConf C **030908**, MODT002 (2003), https://www.slac.stanford.edu/econf/C030908/.
[66] J. M. Blatt and V. F. Weisskopf, *Theoretical Nuclear Physics* (Springer, New York, 1952).
[67] S. S. Wilks, The large-sample distribution of the likelihood ratio for testing composite hypotheses, Ann. Math. Stat. **9**, 60 (1938).
[68] R. Aaij *et al.* (LHCb Collaboration), Precision measurement of D meson mass differences, J. High Energy Phys. 06 (2013) 065.
[69] LHCb Collaboration, 2025, CERN Document Server, https://cds.cern.ch/record/2925371.

Correction: In the abstract, the letter m was missing for the $\Xi_c(3080)$ state and has been inserted.

End Matter

Additional information on multivariate selection—Three sequential multivariate algorithms (MVA) are used to select signal candidates for this analysis. This gives better performance than using a single MVA because the classifiers are tuned to reject the particular background contributions at each stage, and the first two benefit from being trained with real data. The classifiers are selected independently based on the best performance, and are drawn from several different machine learning libraries.

The first MVA maximizes the significance of the ground state Ξ_c^+ signal, discriminating against random three-track combinations that pass the earlier selection criteria. The best performance is obtained using a feed-forward neural network from the TensorFlow and Keras libraries, with a $[n, 32,16,4,1]$ topology, where $n = 29$ is the number of input variables. A leaky rectified linear unit (LeakyReLU) activation function is used for the hidden layers [32,16,4] to improve the performance. The 29 input variables are as follows.

Topological variables (10): Fit χ^2 of the Ξ_c^+ decay vertex; flight distance (FD) of the Ξ_c^+ candidate; FD divided by its uncertainty of the Ξ_c^+ candidate; difference in PV fit χ^2 with and without the Ξ_c^+ included in the fit ($\chi^2_{\rm IP}$); cosine of the direction angle between the Ξ_c^+ displacement and momentum vectors; distance-of-closest-approach between each pair of final-state particles; minimum distance-of-closest-approach value; impact parameter of the proton.

Kinematic variables (2): Ξ_c^+ pseudorapidity; proton transverse momentum.

Particle identification variables (17): For each final-state hadron: The output of LHCb-specific multivariate classifiers used to separate different hadron hypotheses using information from the RICH and other subdetectors, and the output of a separate multivariate algorithm to reject fake tracks from random hit combinations.

The classifier is trained with data, using the sPlot method as described in the main text.

The second MVA maximizes the significance of the $\Xi_c(2645)^0$ signal, discriminating against a background primarily coming from genuine Ξ_c^+ baryons combined with an unrelated pion. The best performance is obtained with a gradient boosted decision tree from the SKLEARN library, using 14 input variables.

Topological variables (6): Reduced χ^2 of the kinematic refit that constrains the pion and Ξ_c^+ to originate from a common vertex; reduced χ^2 of the $\Xi_c(2645)^0$ decay vertex fit; $\chi^2_{\rm IP}$ for the $\Xi_c(2645)^0$ candidate, the pion from the $\Xi_c(2645)^0$ decay, and the Ξ_c^+ candidate.

Kinematic variables (3): $\Xi_c(2645)^0$ momentum; momentum and transverse momentum of the pion from the $\Xi_c(2645)^0$ decay.

Particle identification variables (4): For the pion from the $\Xi_c(2645)^0$ decay, outputs from LHCb-specific multivariate classifiers used to differentiate between pion and other hadron hypotheses, and the output of a separate multivariate algorithm to reject fake tracks from random hit combinations.

Other variables (1): The output of the stage-1 MVA classifier.

This classifier is also trained using the sPlot method with data, as described in the main text.

The third MVA is optimized using the Punzi figure of merit to discriminate the Ξ_c^{**+} signals from a hybrid background including both genuine and fake $\Xi_c(2645)^0$ candidates combined with an unrelated pion. The best performance is obtained with a gradient boosted decision tree from the Catboost library, with 15 input variables.

Topological variables (8): Vertex-fit χ^2 of the Ξ_c^{**+} candidate; $\chi^2_{\rm IP}$ of the Ξ_c^{**+} candidate; $\chi^2_{\rm IP}$ of each of the two pions from the Ξ_c^{**+} decay; FD divided by its uncertainty of the Ξ_c^{**+} candidate; FD divided by its uncertainty of the Ξ_c^+ candidate; reduced χ^2 of the kinematic refit that constrains the Ξ_c^+ candidate and the two accompanying pions to originate from a common vertex; a derived quantity $\chi^2_{\rm IP}(\Xi_c^+)/[\chi^2_{\rm IP}(\Xi_c^+) + \chi^2_{\rm IP}(\pi^+) + \chi^2_{\rm IP}(\pi^-)]$.

Kinematic variables (3): Three quantities derived from the transverse momenta of the Ξ_c^{**+} decay products: $[p_{\rm T}(\Xi_c^+) + p_{\rm T}(\pi^+) + p_{\rm T}(\pi^-)]$; $\min[p_{\rm T}(\pi^+), p_{\rm T}(\pi^-)]$; $p_{\rm T}(\Xi_c^+)/[p_{\rm T}(\Xi_c^+) + p_{\rm T}(\pi^+) + p_{\rm T}(\pi^-)]$.

Particle identification variables (4): For each of the two pions from the Ξ_c^{**+} decay, the value of two LHCb multivariate classifiers, quantifying the confidence in a pion hypothesis and in a fake-track hypothesis, respectively.

The classifier is trained using simulation and control samples in data, as described in the main text.

Mass distributions for wrong-sign samples—To verify that the selection criteria do not cause any distortions of the ΔM distribution, the wrong-sign sample is inspected after applying all requirements. The result is shown in Fig. 4. The overall impact of the selection is to suppress background fairly uniformly across the ΔM range,

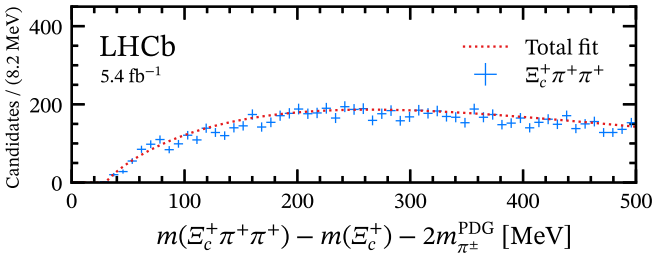

FIG. 4. Distribution of ΔM for candidates from the wrong-sign $\Xi_c^+\pi^+\pi^+$ sample, passing all selection requirements. No peaking behavior is observed. An illustrative fit is also shown using the same function as used for the signal sample.

and there is no indication of any peaking behavior. An illustrative fit is performed with the same background model as used for the signal sample.

Mass difference measurements—In the fit to the ΔM distribution, the peak positions are free parameters, denoted $\delta M(X)$ for state X. The values returned by the fit are

$$\delta M[\Xi_c(2815)^+] = 69.80 \pm 0.03 \pm 0.03 \text{ MeV},$$
$$\delta M[\Xi_c(2923)^+] = 175.95 \pm 0.28 \pm 0.54 \text{ MeV},$$
$$\delta M[\Xi_c(2970)^+] = 221.77 \pm 0.46 \pm 0.48 \text{ MeV},$$
$$\delta M[\Xi_c(3080)^+] = 329.92 \pm 0.72 \pm 1.27 \text{ MeV},$$

where the first uncertainty is statistical and the second is due to experimental systematic effects. These measurements are converted into absolute mass measurements for the excited baryons, as reported in the Letter, by adding the masses of the two charged pions and the Ξ_c^+ baryon (2467.71 ± 0.23 MeV) taken from Ref. [31].

R. Aaij,[38] A. S. W. Abdelmotteleb,[57] C. Abellan Beteta,[51] F. Abudinén,[57] T. Ackernley,[61] A. A. Adefisoye,[69] B. Adeva,[47] M. Adinolfi,[55] P. Adlarson,[83] C. Agapopoulou,[14] C. A. Aidala,[85] Z. Ajaltouni,[11] S. Akar,[11] K. Akiba,[38] P. Albicocco,[28] J. Albrecht,[19,b] F. Alessio,[49] M. Alexander,[60] Z. Aliouche,[63] P. Alvarez Cartelle,[56] R. Amalric,[16] S. Amato,[3] J. L. Amey,[55] Y. Amhis,[14] L. An,[6] L. Anderlini,[27] M. Andersson,[51] A. Andreianov,[44] P. Andreola,[51] M. Andreotti,[26] D. Andreou,[69] A. Anelli,[31,49,c] D. Ao,[7] F. Archilli,[37,d] M. Argenton,[26] S. Arguedas Cuendis,[9,49] A. Artamonov,[44] M. Artuso,[69] E. Aslanides,[13] R. Ataíde Da Silva,[50] M. Atzeni,[65] B. Audurier,[12] D. Bacher,[64] I. Bachiller Perea,[10] S. Bachmann,[22] M. Bachmayer,[50] J. J. Back,[57] P. Baladron Rodriguez,[47] V. Balagura,[15] A. Balboni,[26] W. Baldini,[26] L. Balzani,[19] H. Bao,[7] J. Baptista de Souza Leite,[61] C. Barbero Pretel,[47,12] M. Barbetti,[27] I. R. Barbosa,[70] R. J. Barlow,[63] M. Barnyakov,[25] S. Barsuk,[14] W. Barter,[59] J. Bartz,[69] J. M. Basels,[17] S. Bashir,[40] B. Batsukh,[5] P. B. Battista,[14] A. Bay,[50] A. Beck,[65] M. Becker,[19] F. Bedeschi,[35] I. B. Bediaga,[2] N. A. Behling,[19] S. Belin,[47] K. Belous,[44] I. Belov,[29] I. Belyaev,[36] G. Benane,[13] G. Bencivenni,[28] E. Ben-Haim,[16] A. Berezhnoy,[44] R. Bernet,[51] S. Bernet Andres,[45] A. Bertolin,[33] C. Betancourt,[51] F. Betti,[59] J. Bex,[56] Ia. Bezshyiko,[51] O. Bezshyyko,[84] J. Bhom,[41] M. S. Bieker,[19] N. V. Biesuz,[26] P. Billoir,[16] A. Biolchini,[38] M. Birch,[62] F. C. R. Bishop,[10] A. Bitadze,[63] A. Bizzeti,[27] T. Blake,[57] F. Blanc,[50] J. E. Blank,[19] S. Blusk,[69] V. Bocharnikov,[44] J. A. Boelhauve,[19] O. Boente Garcia,[15] T. Boettcher,[68] A. Bohare,[59] A. Boldyrev,[44] C. S. Bolognani,[80] R. Bolzonella,[26] R. B. Bonacci,[1] N. Bondar,[44,49] A. Bordelius,[49] F. Borgato,[33,49] S. Borghi,[63] M. Borsato,[31,c] J. T. Borsuk,[81] E. Bottalico,[61] S. A. Bouchiba,[50] M. Bovill,[64] T. J. V. Bowcock,[61] A. Boyer,[49] C. Bozzi,[26] J. D. Brandenburg,[86] A. Brea Rodriguez,[50] N. Breer,[19] J. Brodzicka,[41] A. Brossa Gonzalo,[47,a] J. Brown,[61] D. Brundu,[32] E. Buchanan,[59] L. Buonincontri,[33,e] M. Burgos Marcos,[80] A. T. Burke,[63] C. Burr,[49] J. S. Butter,[56] J. Buytaert,[49] W. Byczynski,[49] S. Cadeddu,[32] H. Cai,[74] A. Caillet,[16] R. Calabrese,[26,f] S. Calderon Ramirez,[9] L. Calefice,[46] S. Cali,[28] M. Calvi,[31,c] M. Calvo Gomez,[45] P. Camargo Magalhaes,[2,g] J. I. Cambon Bouzas,[47] P. Campana,[28] D. H. Campora Perez,[80] A. F. Campoverde Quezada,[7] S. Capelli,[31] L. Capriotti,[26] R. Caravaca-Mora,[9] A. Carbone,[25,h] L. Carcedo Salgado,[47] R. Cardinale,[29,i] A. Cardini,[32] P. Carniti,[31,c] L. Carus,[22] A. Casais Vidal,[65] R. Caspary,[22] G. Casse,[61] M. Cattaneo,[49] G. Cavallero,[26,49] V. Cavallini,[26,f] S. Celani,[22] S. Cesare,[30,j] A. J. Chadwick,[61] I. Chahrour,[85] H. Chang,[4,k] M. Charles,[16] Ph. Charpentier,[49] E. Chatzianagnostou,[38] M. Chefdeville,[10] C. Chen,[56] S. Chen,[5] Z. Chen,[7] A. Chernov,[41] S. Chernyshenko,[53] X. Chiotopoulos,[80] V. Chobanova,[82] M. Chrzaszcz,[41] A. Chubykin,[44] V. Chulikov,[28,36] P. Ciambrone,[28] X. Cid Vidal,[47] G. Ciezarek,[49] P. Cifra,[49] P. E. L. Clarke,[59] M. Clemencic,[49] H. V. Cliff,[56] J. Closier,[49] C. Cocha Toapaxi,[22] V. Coco,[49] J. Cogan,[13] E. Cogneras,[11] L. Cojocariu,[43] S. Collaviti,[50] P. Collins,[49] T. Colombo,[49] M. Colonna,[19] A. Comerma-Montells,[46] L. Congedo,[24] A. Contu,[32] N. Cooke,[60] C. Coronel,[66] I. Corredoira,[12] A. Correia,[16] G. Corti,[49] J. Cottee Meldrum,[55] B. Couturier,[49] D. C. Craik,[51] M. Cruz Torres,[2] E. Curras Rivera,[50] R. Currie,[59] C. L. Da Silva,[68] S. Dadabaev,[44] L. Dai,[71] X. Dai,[4] E. Dall'Occo,[49]

J. Dalseno,[82] C. D'Ambrosio,[49] J. Daniel,[11] P. d'Argent,[24] G. Darze,[3] A. Davidson,[57] J. E. Davies,[63] O. De Aguiar Francisco,[63] C. De Angelis,[32,l] F. De Benedetti,[49] J. de Boer,[38] K. De Bruyn,[79] S. De Capua,[63] M. De Cian,[22] U. De Freitas Carneiro Da Graca,[2,m] E. De Lucia,[28] J. M. De Miranda,[2] L. De Paula,[3] M. De Serio,[24,n] P. De Simone,[28] F. De Vellis,[19] J. A. de Vries,[80] F. Debernardis,[24] D. Decamp,[10] V. Dedu,[13] S. Dekkers,[1] L. Del Buono,[16] B. Delaney,[65] H.-P. Dembinski,[19] J. Deng,[8] V. Denysenko,[51] O. Deschamps,[11] F. Dettori,[32,l] B. Dey,[77] P. Di Nezza,[28] I. Diachkov,[44] S. Didenko,[44] S. Ding,[69] L. Dittmann,[22] V. Dobishuk,[53] A. D. Docheva,[60] C. Dong,[4,k] A. M. Donohoe,[23] F. Dordei,[32] A. C. dos Reis,[2] A. D. Dowling,[69] W. Duan,[72] P. Duda,[81] M. W. Dudek,[41] L. Dufour,[49] V. Duk,[34] P. Durante,[49] M. M. Duras,[81] J. M. Durham,[68] O. D. Durmus,[77] A. Dziurda,[41] A. Dzyuba,[44] S. Easo,[58] E. Eckstein,[18] U. Egede,[1] A. Egorychev,[44] V. Egorychev,[44] S. Eisenhardt,[59] E. Ejopu,[63] L. Eklund,[83] M. Elashri,[66] J. Ellbracht,[19] S. Ely,[62] A. Ene,[43] J. Eschle,[69] S. Esen,[22] T. Evans,[38] F. Fabiano,[32] S. Faghih,[66] L. N. Falcao,[2] Y. Fan,[7] B. Fang,[7] L. Fantini,[34,49,o] M. Faria,[50] K. Farmer,[59] D. Fazzini,[31,c] L. Felkowski,[81] M. Feng,[5,7] M. Feo,[2] A. Fernandez Casani,[48] M. Fernandez Gomez,[47] A. D. Fernez,[67] F. Ferrari,[25,h] F. Ferreira Rodrigues,[3] M. Ferrillo,[51] M. Ferro-Luzzi,[49] S. Filippov,[44] R. A. Fini,[24] M. Fiorini,[26,f] M. Firlej,[40] K. L. Fischer,[64] D. S. Fitzgerald,[85] C. Fitzpatrick,[63] T. Fiutowski,[40] F. Fleuret,[15] M. Fontana,[25] L. F. Foreman,[63] R. Forty,[49] D. Foulds-Holt,[56] V. Franco Lima,[3] M. Franco Sevilla,[67] M. Frank,[49] E. Franzoso,[26,f] G. Frau,[63] C. Frei,[49] D. A. Friday,[63] J. Fu,[7] Q. Führing,[19,56,b] Y. Fujii,[1] T. Fulghesu,[13] E. Gabriel,[38] G. Galati,[24] M. D. Galati,[38] A. Gallas Torreira,[47] D. Galli,[25,h] S. Gambetta,[59] M. Gandelman,[3] P. Gandini,[30] B. Ganie,[63] H. Gao,[7] R. Gao,[64] T. Q. Gao,[56] Y. Gao,[8] Y. Gao,[6] Y. Gao,[8] L. M. Garcia Martin,[50] P. Garcia Moreno,[46] J. García Pardiñas,[49] P. Gardner,[67] K. G. Garg,[8] L. Garrido,[46] C. Gaspar,[49] A. Gavrikov,[33] L. L. Gerken,[19] E. Gersabeck,[63] M. Gersabeck,[20] T. Gershon,[57] S. Ghizzo,[29,i] Z. Ghorbanimoghaddam,[55] L. Giambastiani,[33,e] F. I. Giasemis,[16,p] V. Gibson,[56] H. K. Giemza,[42] A. L. Gilman,[64] M. Giovannetti,[28] A. Gioventù,[46] L. Girardey,[63,58] C. Giugliano,[26,f] M. A. Giza,[41] F. C. Glaser,[14,22] V. V. Gligorov,[16,49] C. Göbel,[70] L. Golinka-Bezshyyko,[84] E. Golobardes,[45] D. Golubkov,[44] A. Golutvin,[62,49] S. Gomez Fernandez,[46] W. Gomulka,[40] F. Goncalves Abrantes,[64] M. Goncerz,[41] G. Gong,[4,k] J. A. Gooding,[19] I. V. Gorelov,[44] C. Gotti,[31] E. Govorkova,[65] J. P. Grabowski,[18] L. A. Granado Cardoso,[49] E. Graugés,[46] E. Graverini,[50,q] L. Grazette,[57] G. Graziani,[27] A. T. Grecu,[43] L. M. Greeven,[38] N. A. Grieser,[66] L. Grillo,[60] S. Gromov,[44] C. Gu,[15] M. Guarise,[26] L. Guerry,[11] V. Guliaeva,[44] P. A. Günther,[22] A.-K. Guseinov,[50] E. Gushchin,[44] Y. Guz,[6,49] T. Gys,[49] K. Habermann,[18] T. Hadavizadeh,[1] C. Hadjivasiliou,[67] G. Haefeli,[50] C. Haen,[49] G. Hallett,[57] M. M. Halvorsen,[49] P. M. Hamilton,[67] J. Hammerich,[61] Q. Han,[33] X. Han,[22,49] S. Hansmann-Menzemer,[22] L. Hao,[7] N. Harnew,[64] T. H. Harris,[1] M. Hartmann,[14] S. Hashmi,[40] J. He,[7,r] F. Hemmer,[49] C. Henderson,[66] R. D. L. Henderson,[1,57] A. M. Hennequin,[49] K. Hennessy,[61] L. Henry,[50] J. Herd,[62] P. Herrero Gascon,[22] J. Heuel,[17] A. Hicheur,[3] G. Hijano Mendizabal,[51] J. Horswill,[63] R. Hou,[8] Y. Hou,[11] N. Howarth,[61] J. Hu,[72] W. Hu,[6] X. Hu,[4,k] W. Huang,[7] W. Hulsbergen,[38] R. J. Hunter,[57] M. Hushchyn,[44] D. Hutchcroft,[61] M. Idzik,[40] D. Ilin,[44] P. Ilten,[66] A. Inglessi,[44] A. Iniukhin,[44] A. Ishteev,[44] K. Ivshin,[44] R. Jacobsson,[49] H. Jage,[17] S. J. Jaimes Elles,[75,49,48] S. Jakobsen,[49] E. Jans,[38] B. K. Jashal,[48] A. Jawahery,[67] V. Jevtic,[19,b] E. Jiang,[67] X. Jiang,[5,7] Y. Jiang,[7] Y. J. Jiang,[6] M. John,[64] A. John Rubesh Rajan,[23] D. Johnson,[54] C. R. Jones,[56] T. P. Jones,[57] S. Joshi,[42] B. Jost,[49] J. Juan Castella,[56] N. Jurik,[49] I. Juszczak,[41] D. Kaminaris,[50] S. Kandybei,[52] M. Kane,[59] Y. Kang,[4,k] C. Kar,[11] M. Karacson,[49] D. Karpenkov,[44] A. Kauniskangas,[50] J. W. Kautz,[66] M. K. Kazanecki,[41] F. Keizer,[49] M. Kenzie,[56] T. Ketel,[38] B. Khanji,[69] A. Kharisova,[44] S. Kholodenko,[35,49] G. Khreich,[14] T. Kirn,[17] V. S. Kirsebom,[31,c] O. Kitouni,[65] S. Klaver,[39] N. Kleijne,[35,s] K. Klimaszewski,[42] M. R. Kmiec,[42] S. Koliiev,[53] L. Kolk,[19] A. Konoplyannikov,[6] P. Kopciewicz,[49] P. Koppenburg,[38] A. Korchin,[52] M. Korolev,[44] I. Kostiuk,[38] O. Kot,[53] S. Kotriakhova, A. Kozachuk,[44] P. Kravchenko,[44] L. Kravchuk,[44] M. Kreps,[57] P. Krokovny,[44] W. Krupa,[69] W. Krzemien,[42] O. Kshyvanskyi,[53] S. Kubis,[81] M. Kucharczyk,[41] V. Kudryavtsev,[44] E. Kulikova,[44] A. Kupsc,[83] V. Kushnir,[52] B. K. Kutsenko,[13] I. Kyryllin,[52] D. Lacarrere,[49] P. Laguarta Gonzalez,[46] A. Lai,[32] A. Lampis,[32] D. Lancierini,[62] C. Landesa Gomez,[47] J. J. Lane,[1] R. Lane,[55] G. Lanfranchi,[28] C. Langenbruch,[22] J. Langer,[19] O. Lantwin,[44] T. Latham,[57] F. Lazzari,[35,49,q] C. Lazzeroni,[54] R. Le Gac,[13] H. Lee,[61] R. Lefèvre,[11] A. Leflat,[44] S. Legotin,[44] M. Lehuraux,[57] E. Lemos Cid,[49] O. Leroy,[13] T. Lesiak,[41] E. D. Lesser,[49] B. Leverington,[22] A. Li,[4,k] C. Li,[4]

C. Li,[13] H. Li,[72] J. Li,[8] K. Li,[8] L. Li,[63] M. Li,[8] P. Li,[7] P.-R. Li,[73] Q. Li,[5,7] S. Li,[8] T. Li,[71] T. Li,[72] Y. Li,[8] Y. Li,[5] Z. Lian,[4,k] X. Liang,[69] S. Libralon,[48] C. Lin,[7] T. Lin,[58] R. Lindner,[49] H. Linton,[62] V. Lisovskyi,[50] R. Litvinov,[32,49] D. Liu,[8] F. L. Liu,[1] G. Liu,[72] K. Liu,[73] S. Liu,[5,7] W. Liu,[8] Y. Liu,[59] Y. Liu,[73] Y. L. Liu,[62] G. Loachamin Ordonez,[70] A. Lobo Salvia,[46] A. Loi,[32] T. Long,[56] J. H. Lopes,[3] A. Lopez Huertas,[46] S. López Soliño,[47] Q. Lu,[15] C. Lucarelli,[27,t] D. Lucchesi,[33,e] M. Lucio Martinez,[80] V. Lukashenko,[38,53] Y. Luo,[6] A. Lupato,[33,u] E. Luppi,[26,f] K. Lynch,[23] X.-R. Lyu,[7] G. M. Ma,[4,k] S. Maccolini,[19] F. Machefert,[14] F. Maciuc,[43] B. Mack,[69] I. Mackay,[64] L. M. Mackey,[69] L. R. Madhan Mohan,[56] M. J. Madurai,[54] A. Maevskiy,[44] D. Magdalinski,[38] D. Maisuzenko,[44] J. J. Malczewski,[41] S. Malde,[64] L. Malentacca,[49] A. Malinin,[44] T. Maltsev,[44] G. Manca,[32,l] G. Mancinelli,[13] C. Mancuso,[30] R. Manera Escalero,[46] F. M. Manganella,[37] D. Manuzzi,[25] D. Marangotto,[30] J. F. Marchand,[10] R. Marchevski,[50] U. Marconi,[25] E. Mariani,[16] S. Mariani,[49] C. Marin Benito,[46] J. Marks,[22] A. M. Marshall,[55] L. Martel,[64] G. Martelli,[34,o] G. Martellotti,[36] L. Martinazzoli,[49] M. Martinelli,[31,c] D. Martinez Gomez,[79] D. Martinez Santos,[82] F. Martinez Vidal,[48] A. Martorell i Granollers,[45] A. Massafferri,[2] R. Matev,[49] A. Mathad,[49] V. Matiunin,[44] C. Matteuzzi,[69] K. R. Mattioli,[15] A. Mauri,[62] E. Maurice,[15] J. Mauricio,[46] P. Mayencourt,[50] J. Mazorra de Cos,[48] M. Mazurek,[42] M. McCann,[62] T. H. McGrath,[63] N. T. McHugh,[60] A. McNab,[63] R. McNulty,[23] B. Meadows,[66] G. Meier,[19] D. Melnychuk,[42] F. M. Meng,[4,k] M. Merk,[38,80] A. Merli,[50] L. Meyer Garcia,[67] D. Miao,[5,7] H. Miao,[7] M. Mikhasenko,[76] D. A. Milanes,[75,v] A. Minotti,[31,c] E. Minucci,[28] T. Miralles,[11] B. Mitreska,[19] D. S. Mitzel,[19] A. Modak,[58] L. Moeser,[19] R. A. Mohammed,[64] R. D. Moise,[17] E. F. Molina Cardenas,[85] T. Mombächer,[49] M. Monk,[57,1] S. Monteil,[11] A. Morcillo Gomez,[47] G. Morello,[28] M. J. Morello,[35,s] M. P. Morgenthaler,[22] J. Moron,[40] W. Morren,[38] A. B. Morris,[49] A. G. Morris,[13] R. Mountain,[69] H. Mu,[4,k] Z. M. Mu,[6] E. Muhammad,[57] F. Muheim,[59] M. Mulder,[79] K. Müller,[51] F. Muñoz-Rojas,[9] R. Murta,[62] V. Mytrochenko,[52] P. Naik,[61] T. Nakada,[50] R. Nandakumar,[58] T. Nanut,[49] I. Nasteva,[3] M. Needham,[59] E. Nekrasova,[44] N. Neri,[30,j] S. Neubert,[18] N. Neufeld,[49] P. Neustroev,[44] J. Nicolini,[49] D. Nicotra,[80] E. M. Niel,[49] N. Nikitin,[44] Q. Niu,[73] P. Nogarolli,[3] P. Nogga,[18] C. Normand,[55] J. Novoa Fernandez,[47] G. Nowak,[66] C. Nunez,[85] H. N. Nur,[60] A. Oblakowska-Mucha,[40] V. Obraztsov,[44] T. Oeser,[17] S. Okamura,[26,f] A. Okhotnikov,[44] O. Okhrimenko,[53] R. Oldeman,[32,l] F. Oliva,[59] M. Olocco,[19] C. J. G. Onderwater,[80] R. H. O'Neil,[49] D. Osthues,[19] J. M. Otalora Goicochea,[3] P. Owen,[51] A. Oyanguren,[48] O. Ozcelik,[59] F. Paciolla,[35,w] A. Padee,[42] K. O. Padeken,[18] B. Pagare,[57] T. Pajero,[49] A. Palano,[24] M. Palutan,[28] X. Pan,[4,k] G. Panshin,[5] L. Paolucci,[57] A. Papanestis,[58,49] M. Pappagallo,[24,n] L. L. Pappalardo,[26] C. Pappenheimer,[66] C. Parkes,[63] D. Parmar,[76] B. Passalacqua,[26,f] G. Passaleva,[27] D. Passaro,[35,49,s] A. Pastore,[24] M. Patel,[62] J. Patoc,[64] C. Patrignani,[25,h] A. Paul,[69] C. J. Pawley,[80] A. Pellegrino,[38] J. Peng,[5,7] M. Pepe Altarelli,[28] S. Perazzini,[25] D. Pereima,[44] H. Pereira Da Costa,[68] A. Pereiro Castro,[47] P. Perret,[11] A. Perrevoort,[79] A. Perro,[49,13] M. J. Peters,[66] K. Petridis,[55] A. Petrolini,[29,i] J. P. Pfaller,[66] H. Pham,[69] L. Pica,[35] M. Piccini,[34] L. Piccolo,[32] B. Pietrzyk,[10] G. Pietrzyk,[14] R. N. Pilato,[61] D. Pinci,[36] F. Pisani,[49] M. Pizzichemi,[31,49,c] V. Placinta,[43] M. Plo Casasus,[47] T. Poeschl,[49] F. Polci,[16] M. Poli Lener,[28] A. Poluektov,[13] N. Polukhina,[44] I. Polyakov,[63] E. Polycarpo,[3] S. Ponce,[49] D. Popov,[7,49] S. Poslavskii,[44] K. Prasanth,[59] C. Prouve,[82] D. Provenzano,[32,l] V. Pugatch,[53] G. Punzi,[35,q] S. Qasim,[51] Q. Q. Qian,[6] W. Qian,[7] N. Qin,[4,k] S. Qu,[4,k] R. Quagliani,[49] R. I. Rabadan Trejo,[57] J. H. Rademacker,[55] M. Rama,[35] M. Ramírez García,[85] V. Ramos De Oliveira,[70] M. Ramos Pernas,[57] M. S. Rangel,[3] F. Ratnikov,[44] G. Raven,[39] M. Rebollo De Miguel,[48] F. Redi,[30,u] J. Reich,[55] F. Reiss,[20] Z. Ren,[7] P. K. Resmi,[64] M. Ribalda Galvez,[46] R. Ribatti,[50] G. Ricart,[15,12] D. Riccardi,[35,s] S. Ricciardi,[58] K. Richardson,[65] M. Richardson-Slipper,[59] K. Rinnert,[61] P. Robbe,[14,49] G. Robertson,[60] E. Rodrigues,[61] A. Rodriguez Alvarez,[46] E. Rodriguez Fernandez,[47] J. A. Rodriguez Lopez,[75] E. Rodriguez Rodriguez,[49] J. Roensch,[19] A. Rogachev,[44] A. Rogovskiy,[58] D. L. Rolf,[19] P. Roloff,[49] V. Romanovskiy,[66] A. Romero Vidal,[47] G. Romolini,[26] F. Ronchetti,[50] T. Rong,[6] M. Rotondo,[28] S. R. Roy,[22] M. S. Rudolph,[69] M. Ruiz Diaz,[22] R. A. Ruiz Fernandez,[47] J. Ruiz Vidal,[80] J. Ryzka,[40] J. J. Saavedra-Arias,[9] J. J. Saborido Silva,[47] R. Sadek,[15] N. Sagidova,[44] D. Sahoo,[77] N. Sahoo,[54] B. Saitta,[32,l] M. Salomoni,[31,49,c] I. Sanderswood,[48] R. Santacesaria,[36] C. Santamarina Rios,[47] M. Santimaria,[28] L. Santoro,[2] E. Santovetti,[37] A. Saputi,[26,49] D. Saranin,[44] A. Sarnatskiy,[79] G. Sarpis,[59] M. Sarpis,[78] C. Satriano,[36,x] A. Satta,[37] M. Saur,[73] D. Savrina,[44] H. Sazak,[17] F. Sborzacchi,[49,28] A. Scarabotto,[19] S. Schael,[17] S. Scherl,[61] M. Schiller,[60] H. Schindler,[49] M. Schmelling,[21] B. Schmidt,[49]

S. Schmitt,[17] H. Schmitz,[18] O. Schneider,[50] A. Schopper,[62] N. Schulte,[19] S. Schulte,[50] M. H. Schune,[14] G. Schwering,[17] B. Sciascia,[28] A. Sciuccati,[49] I. Segal,[76] S. Sellam,[47] A. Semennikov,[44] T. Senger,[51] M. Senghi Soares,[39] A. Sergi,[29,i] N. Serra,[51] L. Sestini,[27] A. Seuthe,[19] Y. Shang,[6] D. M. Shangase,[85] M. Shapkin,[44] R. S. Sharma,[69] I. Shchemerov,[44] L. Shchutska,[50] T. Shears,[61] L. Shekhtman,[44] Z. Shen,[38] S. Sheng,[5,7] V. Shevchenko,[44] B. Shi,[7] Q. Shi,[7] Y. Shimizu,[14] E. Shmanin,[25] R. Shorkin,[44] J. D. Shupperd,[69] R. Silva Coutinho,[69] G. Simi,[33,e] S. Simone,[24,n] M. Singha,[77] N. Skidmore,[57] T. Skwarnicki,[69] M. W. Slater,[54] E. Smith,[65] K. Smith,[68] M. Smith,[62] A. Snoch,[38] L. Soares Lavra,[59] M. D. Sokoloff,[66] F. J. P. Soler,[60] A. Solomin,[55] A. Solovev,[44] I. Solovyev,[44] N. S. Sommerfeld,[18] R. Song,[1] Y. Song,[50] Y. Song,[4,k] Y. S. Song,[6] F. L. Souza De Almeida,[69] B. Souza De Paula,[3] E. Spadaro Norella,[29,i] E. Spedicato,[25] J. G. Speer,[19] E. Spiridenkov,[44] P. Spradlin,[60] V. Sriskaran,[49] F. Stagni,[49] M. Stahl,[76] S. Stahl,[49] S. Stanislaus,[64] M. Stefaniak,[86] E. N. Stein,[49] O. Steinkamp,[51] O. Stenyakin,[44] H. Stevens,[19] D. Strekalina,[44] Y. Su,[7] F. Suljik,[64] J. Sun,[32] L. Sun,[74] D. Sundfeld,[2] W. Sutcliffe,[51] K. Swientek,[40] F. Swystun,[56] A. Szabelski,[42] T. Szumlak,[40] Y. Tan,[4,k] Y. Tang,[74] M. D. Tat,[22] A. Terentev,[44] F. Terzuoli,[35,49,w] F. Teubert,[49] E. Thomas,[49] D. J. D. Thompson,[54] H. Tilquin,[62] V. Tisserand,[11] S. T'Jampens,[10] M. Tobin,[5,49] L. Tomassetti,[26,f] G. Tonani,[30,j] X. Tong,[6] T. Tork,[30] D. Torres Machado,[2] L. Toscano,[19] D. Y. Tou,[4,k] C. Trippl,[45] G. Tuci,[22] N. Tuning,[38] L. H. Uecker,[22] A. Ukleja,[40] D. J. Unverzagt,[22] A. Upadhyay,[77] B. Urbach,[59] A. Usachov,[39] A. Ustyuzhanin,[44] U. Uwer,[22] V. Vagnoni,[25] V. Valcarce Cadenas,[47] G. Valenti,[25] N. Valls Canudas,[49] J. van Eldik,[49] H. Van Hecke,[68] E. van Herwijnen,[62] C. B. Van Hulse,[47,y] R. Van Laak,[50] M. van Veghel,[38] G. Vasquez,[51] R. Vazquez Gomez,[46] P. Vazquez Regueiro,[47] C. Vázquez Sierra,[82] S. Vecchi,[26] J. J. Velthuis,[55] M. Veltri,[27,z] A. Venkateswaran,[50] M. Verdoglia,[32] M. Vesterinen,[57] D. Vico Benet,[64] P. Vidrier Villalba,[46] M. Vieites Diaz,[47] X. Vilasis-Cardona,[45] E. Vilella Figueras,[61] A. Villa,[25] P. Vincent,[16] B. Vivacqua,[3] F. C. Volle,[54] D. vom Bruch,[13] N. Voropaev,[44] K. Vos,[80] C. Vrahas,[59] J. Wagner,[19] J. Walsh,[35] E. J. Walton,[1,57] G. Wan,[6] A. Wang,[7] C. Wang,[22] G. Wang,[8] H. Wang,[73] J. Wang,[6] J. Wang,[5] J. Wang,[4,k] J. Wang,[74] M. Wang,[49] N. W. Wang,[7] R. Wang,[55] X. Wang,[8] X. Wang,[72] X. W. Wang,[62] Y. Wang,[6] Y. W. Wang,[73] Z. Wang,[14] Z. Wang,[4,k] Z. Wang,[30] J. A. Ward,[57,1] M. Waterlaat,[49] N. K. Watson,[54] D. Websdale,[62] Y. Wei,[6] J. Wendel,[82] B. D. C. Westhenry,[55] C. White,[56] M. Whitehead,[60] E. Whiter,[54] A. R. Wiederhold,[63] D. Wiedner,[19] G. Wilkinson,[64] M. K. Wilkinson,[66] M. Williams,[65] M. J. Williams,[49] M. R. J. Williams,[59] R. Williams,[56] Z. Williams,[55] F. F. Wilson,[58] M. Winn,[12] W. Wislicki,[42] M. Witek,[41] L. Witola,[19] G. Wormser,[14] S. A. Wotton,[56] H. Wu,[69] J. Wu,[8] X. Wu,[74] Y. Wu,[6,56] Z. Wu,[7] K. Wyllie,[49] S. Xian,[72] Z. Xiang,[5] Y. Xie,[8] T. X. Xing,[30] A. Xu,[35] L. Xu,[4,k] L. Xu,[4,k] M. Xu,[57] Z. Xu,[49] Z. Xu,[7] Z. Xu,[5] K. Yang,[62] S. Yang,[7] X. Yang,[6] Y. Yang,[29,i] Z. Yang,[6] V. Yeroshenko,[14] H. Yeung,[63] H. Yin,[8] X. Yin,[7] C. Y. Yu,[6] J. Yu,[71] X. Yuan,[5] Y Yuan,[5,7] E. Zaffaroni,[50] M. Zavertyaev,[21] M. Zdybal,[41] F. Zenesini,[25] C. Zeng,[5,7] M. Zeng,[4,k] C. Zhang,[6] D. Zhang,[8] J. Zhang,[7] L. Zhang,[4,k] S. Zhang,[71] S. Zhang,[64] Y. Zhang,[6] Y. Z. Zhang,[4,k] Z. Zhang,[4,k] Y. Zhao,[22] A. Zhelezov,[22] S. Z. Zheng,[6] X. Z. Zheng,[4,k] Y. Zheng,[7] T. Zhou,[6] X. Zhou,[8] Y. Zhou,[7] V. Zhovkovska,[57] L. Z. Zhu,[7] X. Zhu,[4,k] X. Zhu,[8] Y. Zhu,[17] V. Zhukov,[17] J. Zhuo,[48] Q. Zou,[5,7] D. Zuliani,[33,e] and G. Zunica[50]

(LHCb Collaboration)

[1]*School of Physics and Astronomy, Monash University, Melbourne, Australia*
[2]*Centro Brasileiro de Pesquisas Físicas (CBPF), Rio de Janeiro, Brazil*
[3]*Universidade Federal do Rio de Janeiro (UFRJ), Rio de Janeiro, Brazil*
[4]*Department of Engineering Physics, Tsinghua University, Beijing, China*
[5]*Institute of High Energy Physics (IHEP), Beijing, China*
[6]*School of Physics State Key Laboratory of Nuclear Physics and Technology, Peking University, Beijing, China*
[7]*University of Chinese Academy of Sciences, Beijing, China*
[8]*Institute of Particle Physics, Central China Normal University, Wuhan, Hubei, China*
[9]*Consejo Nacional de Rectores (CONARE), San Jose, Costa Rica*
[10]*Université Savoie Mont Blanc, CNRS, IN2P3-LAPP, Annecy, France*
[11]*Université Clermont Auvergne, CNRS/IN2P3, LPC, Clermont-Ferrand, France*

[12]Université Paris-Saclay, Centre d'Etudes de Saclay (CEA), IRFU, Saclay, Gif-Sur-Yvette, France
[13]Aix Marseille Université, CNRS/IN2P3, CPPM, Marseille, France
[14]Université Paris-Saclay, CNRS/IN2P3, IJCLab, Orsay, France
[15]Laboratoire Leprince-Ringuet, CNRS/IN2P3, Ecole Polytechnique, Institut Polytechnique de Paris, Palaiseau, France
[16]LPNHE, Sorbonne Université, Paris Diderot Sorbonne Paris Cité, CNRS/IN2P3, Paris, France
[17]I. Physikalisches Institut, RWTH Aachen University, Aachen, Germany
[18]Universität Bonn—Helmholtz-Institut für Strahlen und Kernphysik, Bonn, Germany
[19]Fakultät Physik, Technische Universität Dortmund, Dortmund, Germany
[20]Physikalisches Institut, Albert-Ludwigs-Universität Freiburg, Freiburg, Germany
[21]Max-Planck-Institut für Kernphysik (MPIK), Heidelberg, Germany
[22]Physikalisches Institut, Ruprecht-Karls-Universität Heidelberg, Heidelberg, Germany
[23]School of Physics, University College Dublin, Dublin, Ireland
[24]INFN Sezione di Bari, Bari, Italy
[25]INFN Sezione di Bologna, Bologna, Italy
[26]INFN Sezione di Ferrara, Ferrara, Italy
[27]INFN Sezione di Firenze, Firenze, Italy
[28]INFN Laboratori Nazionali di Frascati, Frascati, Italy
[29]INFN Sezione di Genova, Genova, Italy
[30]INFN Sezione di Milano, Milano, Italy
[31]INFN Sezione di Milano-Bicocca, Milano, Italy
[32]INFN Sezione di Cagliari, Monserrato, Italy
[33]INFN Sezione di Padova, Padova, Italy
[34]INFN Sezione di Perugia, Perugia, Italy
[35]INFN Sezione di Pisa, Pisa, Italy
[36]INFN Sezione di Roma La Sapienza, Roma, Italy
[37]INFN Sezione di Roma Tor Vergata, Roma, Italy
[38]Nikhef National Institute for Subatomic Physics, Amsterdam, Netherlands
[39]Nikhef National Institute for Subatomic Physics and VU University Amsterdam, Amsterdam, Netherlands
[40]AGH—University of Krakow, Faculty of Physics and Applied Computer Science, Kraków, Poland
[41]Henryk Niewodniczanski Institute of Nuclear Physics Polish Academy of Sciences, Kraków, Poland
[42]National Center for Nuclear Research (NCBJ), Warsaw, Poland
[43]Horia Hulubei National Institute of Physics and Nuclear Engineering, Bucharest-Magurele, Romania
[44]Authors affiliated with an institute formerly covered by a cooperation agreement with CERN
[45]DS4DS, La Salle, Universitat Ramon Llull, Barcelona, Spain
[46]ICCUB, Universitat de Barcelona, Barcelona, Spain
[47]Instituto Galego de Física de Altas Enerxías (IGFAE), Universidade de Santiago de Compostela, Santiago de Compostela, Spain
[48]Instituto de Fisica Corpuscular, Centro Mixto Universidad de Valencia—CSIC, Valencia, Spain
[49]European Organization for Nuclear Research (CERN), Geneva, Switzerland
[50]Institute of Physics, Ecole Polytechnique Fédérale de Lausanne (EPFL), Lausanne, Switzerland
[51]Physik-Institut, Universität Zürich, Zürich, Switzerland
[52]NSC Kharkiv Institute of Physics and Technology (NSC KIPT), Kharkiv, Ukraine
[53]Institute for Nuclear Research of the National Academy of Sciences (KINR), Kyiv, Ukraine
[54]School of Physics and Astronomy, University of Birmingham, Birmingham, United Kingdom
[55]H.H. Wills Physics Laboratory, University of Bristol, Bristol, United Kingdom
[56]Cavendish Laboratory, University of Cambridge, Cambridge, United Kingdom
[57]Department of Physics, University of Warwick, Coventry, United Kingdom
[58]STFC Rutherford Appleton Laboratory, Didcot, United Kingdom
[59]School of Physics and Astronomy, University of Edinburgh, Edinburgh, United Kingdom
[60]School of Physics and Astronomy, University of Glasgow, Glasgow, United Kingdom
[61]Oliver Lodge Laboratory, University of Liverpool, Liverpool, United Kingdom
[62]Imperial College London, London, United Kingdom
[63]Department of Physics and Astronomy, University of Manchester, Manchester, United Kingdom
[64]Department of Physics, University of Oxford, Oxford, United Kingdom
[65]Massachusetts Institute of Technology, Cambridge, Massachusetts, USA
[66]University of Cincinnati, Cincinnati, Ohio, USA
[67]University of Maryland, College Park, Maryland, USA
[68]Los Alamos National Laboratory (LANL), Los Alamos, New Mexico, USA
[69]Syracuse University, Syracuse, New York, USA
[70]Pontifícia Universidade Católica do Rio de Janeiro (PUC-Rio), Rio de Janeiro, Brazil
(associated with Universidade Federal do Rio de Janeiro (UFRJ), Rio de Janeiro, Brazil)

[71]School of Physics and Electronics, Hunan University, Changsha City, China
(associated with Institute of Particle Physics, Central China Normal University, Wuhan, Hubei, China)
[72]Guangdong Provincial Key Laboratory of Nuclear Science, Guangdong-Hong Kong Joint Laboratory of Quantum Matter, Institute of Quantum Matter, South China Normal University, Guangzhou, China
(associated with Department of Engineering Physics, Tsinghua University, Beijing, China)
[73]Lanzhou University, Lanzhou, China
(associated with Institute of High Energy Physics (IHEP), Beijing, China)
[74]School of Physics and Technology, Wuhan University, Wuhan, China
(associated with Department of Engineering Physics, Tsinghua University, Beijing, China)
[75]Departamento de Fisica, Universidad Nacional de Colombia, Bogota, Colombia
(associated with LPNHE, Sorbonne Université, Paris Diderot Sorbonne Paris Cité, CNRS/IN2P3, Paris, France)
[76]Ruhr Universitaet Bochum, Fakultaet für Physik und Astronomie, Bochum, Germany
(associated with Fakultät Physik, Technische Universität Dortmund, Dortmund, Germany)
[77]Eotvos Lorand University, Budapest, Hungary
(associated with European Organization for Nuclear Research (CERN), Geneva, Switzerland)
[78]Faculty of Physics, Vilnius University, Vilnius, Lithuania
(associated with Physikalisches Institut, Albert-Ludwigs-Universität Freiburg, Freiburg, Germany)
[79]Van Swinderen Institute, University of Groningen, Groningen, Netherlands
(associated with Nikhef National Institute for Subatomic Physics, Amsterdam, Netherlands)
[80]Universiteit Maastricht, Maastricht, Netherlands
(associated with Nikhef National Institute for Subatomic Physics, Amsterdam, Netherlands)
[81]Tadeusz Kosciuszko Cracow University of Technology, Cracow, Poland
(associated with Henryk Niewodniczanski Institute of Nuclear Physics Polish Academy of Sciences, Kraków, Poland)
[82]Universidade da Coruña, A Coruña, Spain
(associated with DS4DS, La Salle, Universitat Ramon Llull, Barcelona, Spain)
[83]Department of Physics and Astronomy, Uppsala University, Uppsala, Sweden
(associated with School of Physics and Astronomy, University of Glasgow, Glasgow, United Kingdom)
[84]Taras Schevchenko University of Kyiv, Faculty of Physics, Kyiv, Ukraine
(associated with Université Paris-Saclay, CNRS/IN2P3, IJCLab, Orsay, France)
[85]University of Michigan, Ann Arbor, Michigan, USA (associated with Syracuse University, Syracuse, New York, USA)
[86]Ohio State University, Columbus, Ohio, USA
(associated with Los Alamos National Laboratory (LANL), Los Alamos, New Mexico, USA)

[a]Deceased.
[b]Also at Lamarr Institute for Machine Learning and Artificial Intelligence, Dortmund, Germany.
[c]Also at Università degli Studi di Milano-Bicocca, Milano, Italy.
[d]Also at Università di Roma Tor Vergata, Roma, Italy.
[e]Also at Università di Padova, Padova, Italy.
[f]Also at Università di Ferrara, Ferrara, Italy.
[g]Also at Facultad de Ciencias Fisicas, Madrid, Spain.
[h]Also at Università di Bologna, Bologna, Italy.
[i]Also at Università di Genova, Genova, Italy.
[j]Also at Università degli Studi di Milano, Milano, Italy.
[k]Also at Center for High Energy Physics, Tsinghua University, Beijing, China.
[l]Also at Università di Cagliari, Cagliari, Italy.
[m]Also at Centro Federal de Educacão Tecnológica Celso Suckow da Fonseca, Rio De Janeiro, Brazil.
[n]Also at Università di Bari, Bari, Italy.
[o]Also at Università di Perugia, Perugia, Italy.
[p]Also at LIP6, Sorbonne Université, Paris, France.
[q]Also at Università di Pisa, Pisa, Italy.
[r]Also at Hangzhou Institute for Advanced Study, UCAS, Hangzhou, China.
[s]Also at Scuola Normale Superiore, Pisa, Italy.
[t]Also at Università di Firenze, Firenze, Italy.
[u]Also at Università di Bergamo, Bergamo, Italy.
[v]Also at Universidad de Ingeniería y Tecnología (UTEC), Lima, Peru.
[w]Also at Università di Siena, Siena, Italy.
[x]Also at Università della Basilicata, Potenza, Italy.
[y]Also at Universidad de Alcalá, Alcalá de Henares, Spain.
[z]Also at Università di Urbino, Urbino, Italy.